Title
Unsymmetrical Bimetallic Complexes with MII–(μ-OH)–MIII Cores (MIIMIII = FeIIFeIII, MnIIFeIII, MnIIMnIII): Structural, Magnetic, and Redox Properties

Journal
Inorganic Chemistry, 52(18)

ISSN
0020-1669

Authors
Sano, Yohei
Weitz, Andrew C
Ziller, Joseph W
et al.

Publication Date
2013-09-16

DOI
10.1021/ic401561k

Peer reviewed

Published in final edited form as:
Inorg Chem. 2013 September 16; 52(18): . doi:10.1021/ic401561k.

Unsymmetrical Bimetallic Complexes with M^{II}–(μ-OH)–M^{II} Cores ($M^{II}M^{III}$ = $Fe^{II}Fe^{III}$, $Mn^{II}Fe^{III}$, $Mn^{II}Mn^{III}$): Structural, Magnetic, and Redox Properties

Yohei Sano[†], **Andrew C. Weitz**[‡], **Joseph W. Ziller**[†], **Michael P. Hendrich**[‡], and **A.S. Borovik**[*,†]

[†]Department of Chemistry, University of California–Irvine, 1102 Natural Sciences II, Irvine, California 92697-2025

[‡]Department of Chemistry, Carnegie Mellon University, Pittsburgh, Pennsylvania 15213

Abstract

Heterobimetallic cores are important unit within the active sites of metalloproteins, but are often difficult to duplicate in synthetic systems. We have developed a synthetic approach for the preparation of a complex with a Mn^{II}–(μ-OH)–Fe^{III} core, in which the metal centers have different coordination environments. Structural and physical data support the assignment of this complex as a heterobimetallic system. Comparison with the analogous homobimetallic complexes, those containing Mn^{II}–(μ-OH)–Mn^{III} and Fe^{II}–(μ-OH)–Fe^{III} cores, further supports this assignment.

Transition metal complexes with discrete dinuclear metal cores have important functional consequences in chemical and biological systems. In biology, several examples have been discovered in which both homo- and heterobimetallic centers are present within the active sites of proteins. Many metalloproteins, such as those performed by methanemonoxygenase hydroxylase, hemerythrin, purple acid phosphatases, and ribonucleotide reductases (RNRs), utilize oxo- or hydroxo-bridged homobimetallic cores that contain Fe or Mn ions.[1] More recently, several classes of RNRs have been found to contain heterobimetallic MnFe cores.[2] These enzymes catalyze the reduction of nucleotides to 2′-deoxynucleotides via the activation of dioxygen or hydrogen peroxide and are known to play an essential role in nucleic acid metabolism.[3] The function of most bimetallic active sites in metalloproteins often requires intermediates that contain an open coordination site for binding and activating small molecules.[4]

A variety of $M^{II}M^{III}$ bimetallic synthetic complexes that contain a bridging hydroxo or phenoxo group have been described previously. In many instances, these complexes utilize symmetric dinucleating ligands[5–7] or form coordinatively saturated geometries around each metal center.[8,9] We reported recently that the tetradentate sulfonamide-based tripodal ligand, *N*,*N*′,*N*″-[2,2′,2″-nitrilotris(ethane-2,1-diyl)]tris-(2,4,6-trimethylbenzene-sulfonamido), $[MST]^{3-}$, enforces a 5-coordinate geometry around a transition metal center and contains a second metal ion binding site to form heterobimetallic systems. Using this ligand complexes with [M^{II}–(μ-OH)–M^{III}] cores (M^{II} = Ca, Sr, Ba; M^{III} = Mn, and Fe) were prepared from the activation of dioxygen.[10] We have expanded the scope of our heterobimetallic systems to include two 3*d* transition metal ions (Fe and Mn) in which the metal centers are linked

Corresponding Author: aborovik@uci.edu.

Crystallographic data in CIF format, experimental details, and UV-vis, FTIR, ESI-MS spectra for all complexes. This material is available free of charge via the Internet at http://pubs.acs.org.

through a bridging hydroxo ligand and two sulfonamide groups of the $[M^{III}(OH)MST]^{-}$ complex. The primary coordination sphere of the second metal ion is completed by 1,4,7-trimethyl-1,4,7-triazacyclononane (TMTACN), to form a 6-coordinate metal center.

The preparation of $[TMTACN\supset Mn^{II}–(\mu\text{-}OH)–Fe^{III}MST]^{+}$ (denoted as $[Mn^{II}(OH)Fe^{III}]^{+}$) was achieved via the synthetic route outlined in Scheme 1. The visible absorbance spectrum of the isolated solid showed an absorbance band at λ_{max} (ε_M) = 390 nm (4600) and a broad shoulder at 470 nm (1780 M) (Figure S1). A broad but intense band was observed in the FTIR spectrum at 3244 cm^{-1} that was assigned to the vibration of the O–H bond (Figure S2).[10] The broadness of this band suggests a strong intramolecular H-bond between the hydroxo ligand and the sulfonamide group. The formulation of the solid as $[Mn^{II}(OH)Fe^{III}]^{+}$ was supported by electrospray ionization mass spectrometry (ESI-MS), in which the molecular weight and the experimental isotope pattern matched those calculated for $[Mn^{II}(OH)Fe^{III}]^{+}$ (Figure S3). Using the same synthetic route, $[TMTACN\supset Fe^{II}–(\mu\text{-}OH)–Fe^{III}MST]^{+}$ ($[Fe^{II}(OH)Fe^{III}]^{+}$) and $[TMTACN\supset Mn^{II}–(\mu\text{-}OH)–Mn^{III}MST]^{+}$ ($[Mn^{II}(OH)Mn^{III}]^{+}$) were also prepared and characterized. These homobimetallic complexes served as control systems for $[Mn^{II}(OH)Fe^{III}]^{+}$ and possess properties expected for their formulation. For example, their ESI-MS spectra were consistent with those for homobimetallic complexes (Figure S3). In addition, $[Fe^{II}(OH)Fe^{III}]^{+}$ had a similar absorbance spectrum to $[Mn^{II}(OH)Fe^{III}]^{+}$ with a peak at λ_{max} = 387 nm (6200), which appears to be representative of complexes containing $[Fe^{III}(OH)MST]^{-}$ units (Figure S1).

The molecular structure of $[Mn^{II}(OH)Fe^{III}]^{+}$ was determined by X-ray diffraction methods and revealed the expected heterobimetallic complex (Figure 1). The Fe^{III} center and the Mn^{II} center have different coordination geometries: the Fe^{III} center exhibits a 5-coordinate, N_4O primary coordination sphere with a distorted trigonal bipyramidal geometry. In contrast, the Mn^{II} center has a 6-coordinate, N_3O_3 primary coordination sphere with a distorted octahedral geometry (Table S4). Note that the configuration of the SO_2Ar groups produced a cavity that forms an intramolecular H-bond between the $Fe^{III}–OH–Mn^{II}$ unit and O6 of the $[MST]^{3-}$ ligand with an O1···O6 distance of 2.646(2) Å. The molecular structures of the homobimetallic complexes $[Fe^{II}(OH)Fe^{III}]^{+}$ and $[Mn^{II}(OH)Mn^{III}]^{+}$ were also determined (Figures S4 & S5) and used to support the assignment of $[Mn^{II}(OH)Fe^{III}]^{+}$ as a heterobimetallic species (Table S4). For instance, for M^{II} center, the avg. $M^{II}–N_{TMTACN}$ bond distance is statistically the same in $[Mn^{II}(OH)Mn^{III}]^{+}$ as in $[Mn^{II}(OH)Fe^{III}]^{+}$ (2.277(7) versus 2.279(2) Å); both values are significantly longer than the average bond distance of 2.210(2) Å observed in $[Fe^{II}(OH)Fe^{III}]^{+}$. Moreover, the displacement of M^{III} center from the plane formed by N5, N6, and N7 in $[Mn^{II}(OH)Mn^{III}]^{+}$ and $[Mn^{II}(OH)Fe^{III}]^{+}$ are nearly identical (1.557 versus 1.552 Å), while that found in $[Fe^{II}(OH)Fe^{III}]^{+}$ is 1.471 Å. For M^{III} center, the displacements of M^{III} center from the plane formed by N2, N3, and N4 of $[MST]^{3-}$ are 0.359 Å in $[Mn^{II}(OH)Fe^{III}]^{+}$ and 0.356 Å in $[Fe^{II}(OH)Fe^{III}]^{+}$, yet in $[Mn^{II}(OH)Mn^{III}]^{+}$ this displacement is only 0.286 Å.

Electron paramagnetic resonance (EPR) spectroscopy was used to further probe properties of these complexes. For $[Mn^{II}(OH)Mn^{III}]^{+}$, the EPR spectrum measured at 11 K displayed a signal from an S = 1/2 spin ground state of antiferromagnetically-coupled Mn^{II} and Mn^{III} high-spin centers (Figure 2A). This signal displays an irregular pattern of hyperfine lines from the inequivalent nuclear spins of the two Mn centers. For $[Fe^{II}(OH)Fe^{III}]^{+}$, the EPR spectrum measured at 11 K displayed a rhombic signal with g-values of 1.91, 1.68, and 1.54 (Figure 2B). This type of spectrum is characteristic of complexes with an antiferromagnetically-coupled $Fe^{II}–(\mu\text{-}OH)–Fe^{III}$ core.[5a] For both complexes, spin quantification of the spectra indicated that the signals accounted for the amount of metal used in the reaction. No EPR signals were observed for $[Mn^{II}(OH)Fe^{III}]^{+}$ at a temperature of 4 K. However, at higher temperatures (e.g. 66 K), a signal is observed at g = 11.3 for the

microwave magnetic field oscillating parallel to the static magnetic field (Figure 2C). The absence of signals at low temperature and presence of the parallel-mode signal at higher temperatures is consistent an antiferromagnetic coupling between the two d^5 metal centers in $[Mn^{II}(OH)Fe^{III}]^+$. It is important to recognize that these initial EPR results are consistent with the bimetallic complexes persisting in solution, in which the antiferromagnetic coupling between the metal centers is promoted via the bridging hydroxo ligand.

Electrochemical results further support that the $[M^{II}(OH)M^{III}]$ complexes are assembled in solution. The cyclic voltammograms for each complex exhibits two quasi-reversible one-electron redox processes that are assigned to the $M^{II}M^{II}/M^{II}M^{III}$ and $M^{II}M^{III}/M^{III}M^{III}$ couples (Figure 3). The most striking finding is that the two redox processes observed for the $[Mn^{II}(OH)Fe^{III}]^+$ complex are nearly identical to the analogous redox process in the $[Fe^{II}(OH)Fe^{III}]^+$ and $[Mn^{II}(OH)Mn^{III}]^+$ complexes. Specifically, the $Mn^{II}Fe^{II}/Mn^{II}Fe^{III}$ couple at −0.88 V matches the $Fe^{II}Fe^{II}/Fe^{II}Fe^{III}$ couple at −0.87 V while the $Mn^{II}Fe^{III}/Mn^{III}Fe^{III}$ couple at 0.71 V matches the $Mn^{I\text{-}I}Mn^{III}/Mn^{III}Mn^{III}$ couple at 0.71 V. These results indicate that the Mn^{II} ion resides in the [TMTACN] binding site and the Fe^{III} center is coordinated to the $[MST]^{3-}$ ligand. Furthermore, the separations between the first and second redox process in the $[M^{II}(OH)M^{III}]^+$ systems are extremely large, with differences of 1.59 V, 1.23 V, and 1.18 V for the $[Mn^{II}(OH)Fe^{III}]^+$, $[Fe^{II}(OH)Fe^{III}]^+$, and $[Mn^{II}(OH)Mn^{III}]^+$ complexes. These separations suggest that the mixed-valence $[M^{II}(OH)M^{III}]^+$ species should be relatively stable toward disproportionation.[5–8]

In summary, we have described the preparation and properties of a series of hetero- and homo-bimetallic complexes of Fe and Mn in differing coordination environments. Structural studies confirmed that each complex contains a M^{II}–(μ-OH)–M^{III} core, with the hydroxo ligand also forming an intramolecular H-bond with the $[MST]^{3-}$ ligand. The metal ion cores adopt stable mixed-valent states of $Mn^{II}Fe^{III}$, $Fe^{II}Fe^{III}$, and $Mn^{II}Mn^{III}$, whose assignments are supported by results from EPR spectroscopy that are consistent with antiferromagnetic coupling of the spins through the hydroxo unit. In addition, two quasi-reversible one-electron redox processes corresponding to the $M^{II}M^{II}/M^{II}M^{III}$ and $M^{II}M^{III}/M^{III}M^{III}$ couples were clearly observed with all of the $[M^{II}(OH)M^{III}]^+$ systems via cyclic voltammetry. These results further illustrate the ability of tripodal sulfonamido ligands to form discrete bimetallic complexes.

Supplementary Material

Refer to Web version on PubMed Central for supplementary material.

Acknowledgments

We thank the NIH (GM050781 to ASB; GM77387 to MPH) for financial support of this work.

References

1. Kurtz DM. Chem Rev. 1990; 90:585.Wu AJ, Penner-Hahn JE, Pecoraro VL. Chem Rev. 2004; 104:903. [PubMed: 14871145] and references cited therein Schenk G, Mitic N, Gahan LR, Ollis DL, McCeary RP, Guddat LW. Acc Chem Res. 2012; 45:1593. [PubMed: 22698580]
2. (a) Jiang W, Yun D, Saleh L, Barr EW, Xing G, Hoffart LM, Maslak MA, Krebs C, Bollinger JM. Science. 2007; 316:1188. [PubMed: 17525338] (b) Andersson CS, Hogbom M. Proc Natl Acad Sci USA. 2009; 106:5633. [PubMed: 19321420] (c) Dassama LMK, Boal AK, Krebs C, Rosenzweig AC, Bollinger JM Jr. J Am Chem Soc. 2012; 134:2520. [PubMed: 22242660]
3. (a) Cotruvo JA Jr, Stubbe J. Annu Rev Biochem. 2011; 80:733. [PubMed: 21456967] (b) Tomter AB, Zoppellaro G, Andersen NH, Hersleth H-P, Hammerstad M, Røhr ÅK, Sandvik GK, Strand

KR, Nilsson GE, Bell CB III, Barra A-L, Blasco E, Le Pape L, Solomon EI, Andersson KK. Coord Chem Rev. 2013; 257:3. and references cited therein.

4. (a) Das D, Eser BE, Han J, Sciore A, Marsh ENG. Angew Chem Int Ed. 2011; 50:7148.(b) Hayashi T, Caranto JD, Matsumura H, Kurtz DM Jr, Moënne-Loccoz P. J Am Chem Soc. 2012; 134:6878. [PubMed: 22449095]
5. (a) Borovik AS, Que L, Papaefthymiou V, Muenck E, Taylor LF, Anderson OP. J Am Chem Soc. 1988; 110:1986.(b) Buchanan RM, Mashuta MS, Richardson JF, Webb RJ, Oberhausen KJ, Nanny MA, Hendrickson DN. Inorg Chem. 1990; 29:1299.
6. (a) Borovik AS, Papaefthymiou V, Taylor LF, Anderson OP, Que L. J Am Chem Soc. 1989; 111:6183.(b) Bossek U, Hummel H, Weyhermüller T, Bili E, Wieghardt K. Angew Chem Int Ed. 1996; 34:2642.
7. (a) Diril H, Chang HR, Zhang X, Larsen SK, Potenza JA, Pierpont CG, Schugar HJ, Isied SS, Hendrickson DN. J Am Chem Soc. 1987; 109:6207.(b) Bossek U, Hummel H, Weyhermüller T, Wieghardt K, Russell S, van der Wolf L, Kolb U. Angew Chem Int Ed. 1996; 35:1552.
8. (a) Kanda W, Moneta W, Bardet M, Bernard E, Debaecker N, Laugier J, Bousseksou A, Chardon-Noblat S, Latour JM. Angew Chem Int Ed. 1995; 34:588.(b) Smith SJ, Riley MJ, Noble CJ, Hanson GR, Stranger R, Jayaratne V, Cavigliasso G, Schenk G, Gahan LR. Inorg Chem. 2009; 48:10036. [PubMed: 19852517] (c) Carboni M, Clémancey M, Molton F, Pécaut J, Lebrun C, Dubois L, Blondin G, Latour JM. Inorg Chem. 2012; 51:10447. [PubMed: 22989001]
9. Examples of unsymmetrical heterobimetallic complexes: Neves A, Lanznster M, Bortoluzzi AJ, Perlta RA, Castllano EE, Herrald P, Riley MJ, Schenk G. J Am Chem Soc. 2007; 129:7486. [PubMed: 17518469] de Souza B, Kreft GL, Bortolotto T, Ternzi H, Bortoluzzi AJ, Castllano EE, Perlta RA, Domingos JB, Neves A. Inorg Chem. 2013; 52:3594. [PubMed: 23496379]
10. (a) Park YJ, Ziller JW, Borovik AS. J Am Chem Soc. 2011; 133:9258. [PubMed: 21595481] (b) Park YJ, Cook SA, Sickerman NS, Sano Y, Ziller JW, Borovik AS. Chem Sci. 2013; 4:717. [PubMed: 24058726]

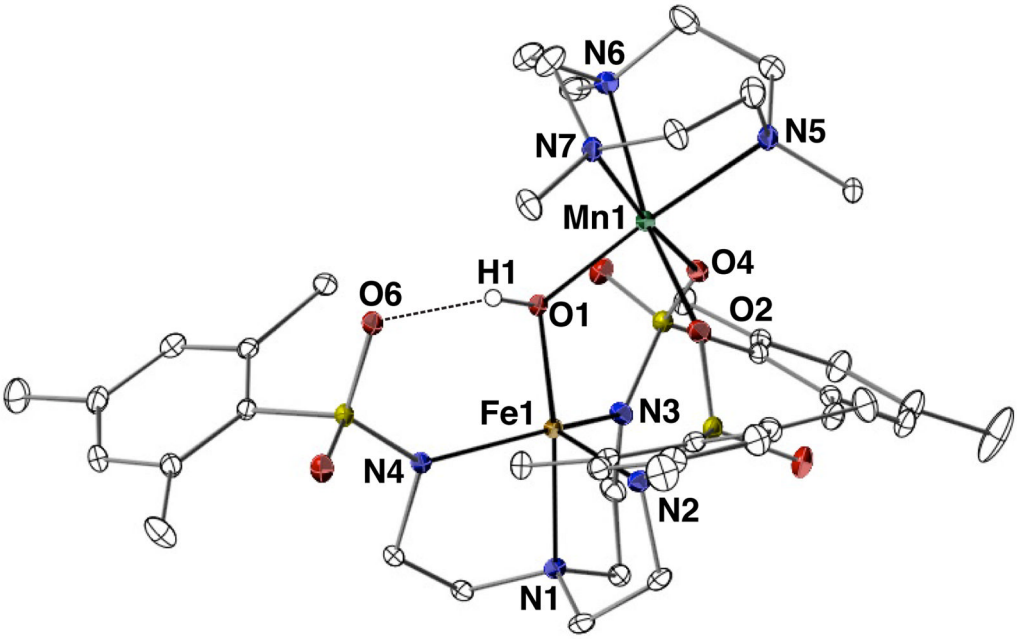

Figure 1.

Thermal ellipsoid diagram depicting the molecular structure of $[Mn^{II}(OH)Fe^{III}]^{+}$. Ellipsoids are drawn at the 50% probability level, and only the hydroxo hydrogen atom is shown for clarity. Selected bond lengths (Å): Fe1–O1, 1.888(1); Fe1–N1, 2.193(2); Fe1–N2, 2.030(2); Fe1–N3, 2.007(2); Fe1–N4, 2.036(2); Fe1···Mn1, 3.447(1); Mn1–O1, 2.048(1); Mn1–N5, 2.268(2); Mn1–N6, 2.276(2); Mn1–N7, 2.294(2); Mn1–O2, 2.196(1); Mn1–O4, 2.187(1); O1···O6, 2.646(2).

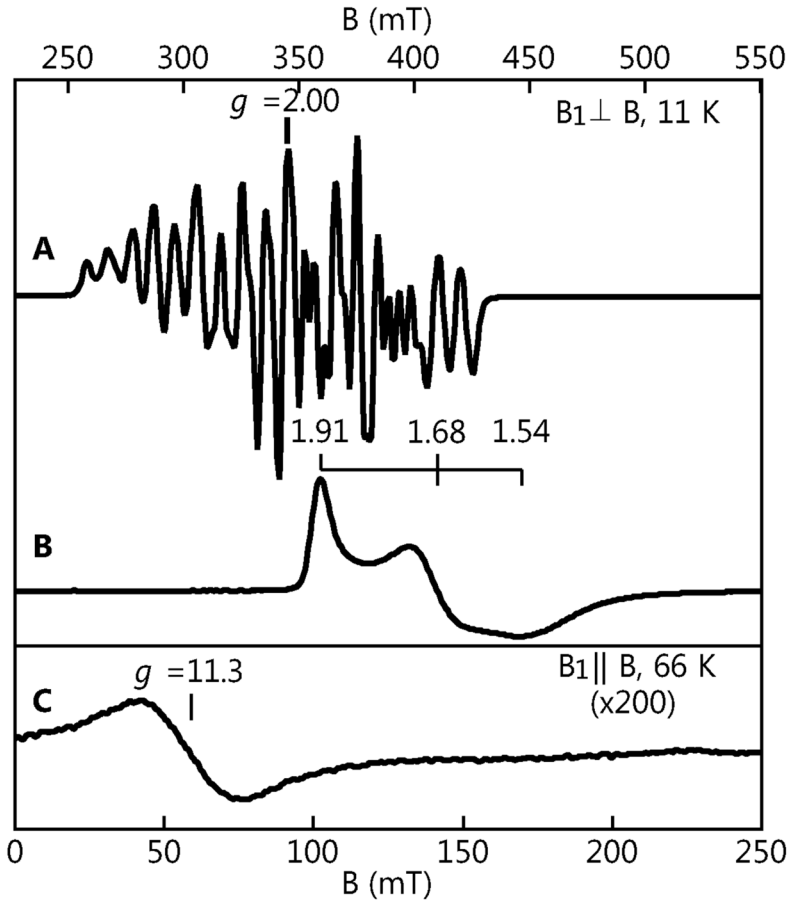

Figure 2.
X-band EPR spectra for (A) $[Mn^{II}(OH)Mn^{III}]^{+}$, (B) $[Fe^{II}(OH)Fe^{III}]^{+}$, and (C) $[Mn^{II}(OH)Fe^{III}]^{+}$.

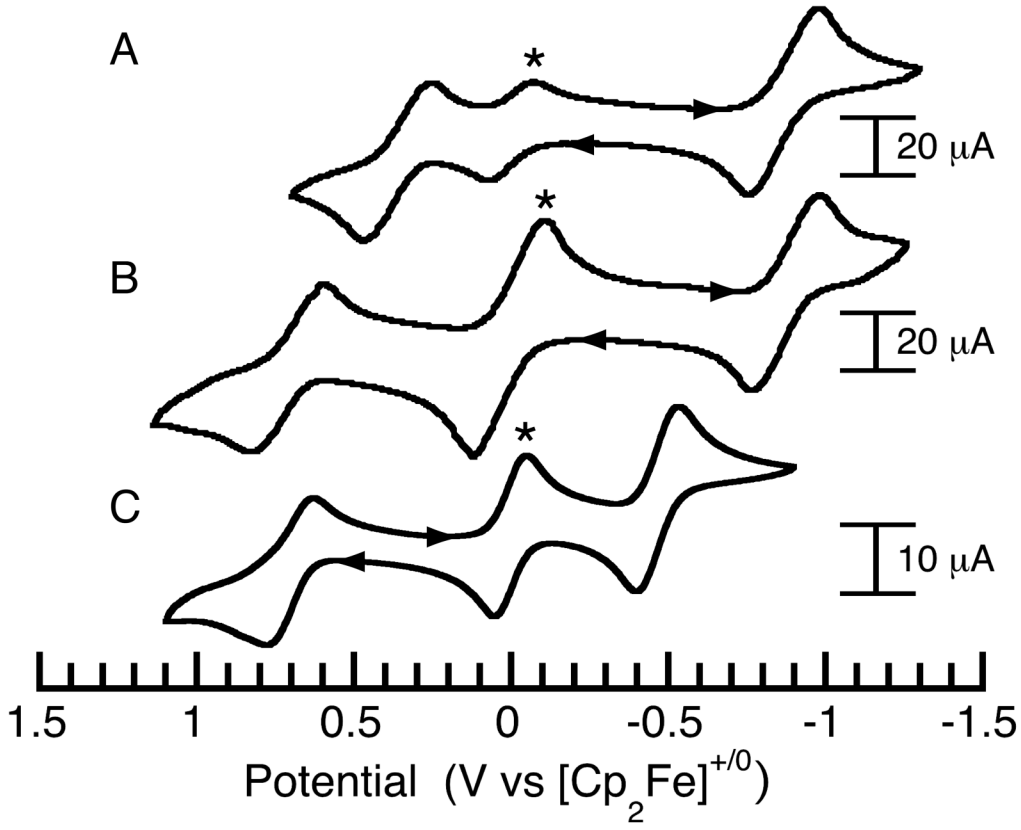

Figure 3.
Cyclic voltammograms of (A) $[Fe^{II}(OH)Fe^{III}]^{+}$, (B) $[Mn^{II}(OH)Fe^{III}]^{+}$, and (C) $[Mn^{II}(OH)Mn^{III}]^{+}$ measured in CH_2Cl_2 (0.1 M TBAP). CVs in (A) and (B) were collected at 100 mV s^{-1}, and in (C) at 20 mV s^{-1} in the presence of $[Cp_2Fe]$ (*).

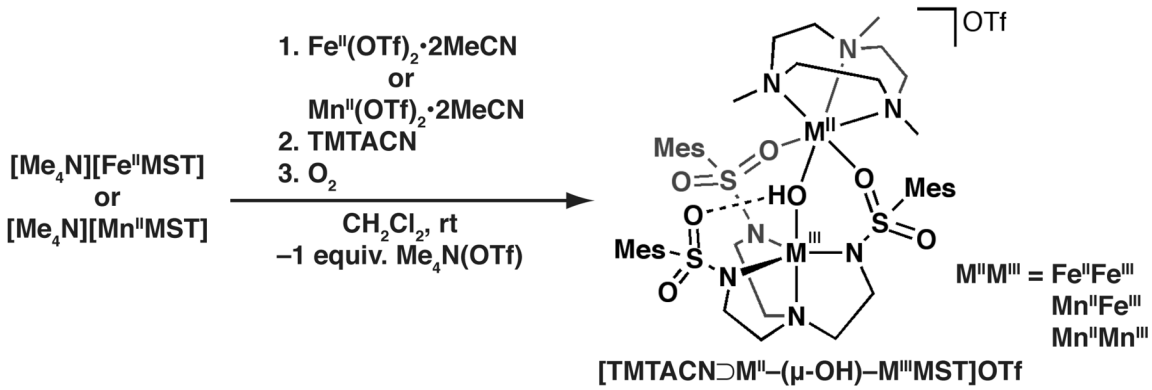

Scheme 1.
Preparative Route to [TMTACN⊃M^{II}–(μ-OH)–M^{III}MST]$^{-}$ complexes.